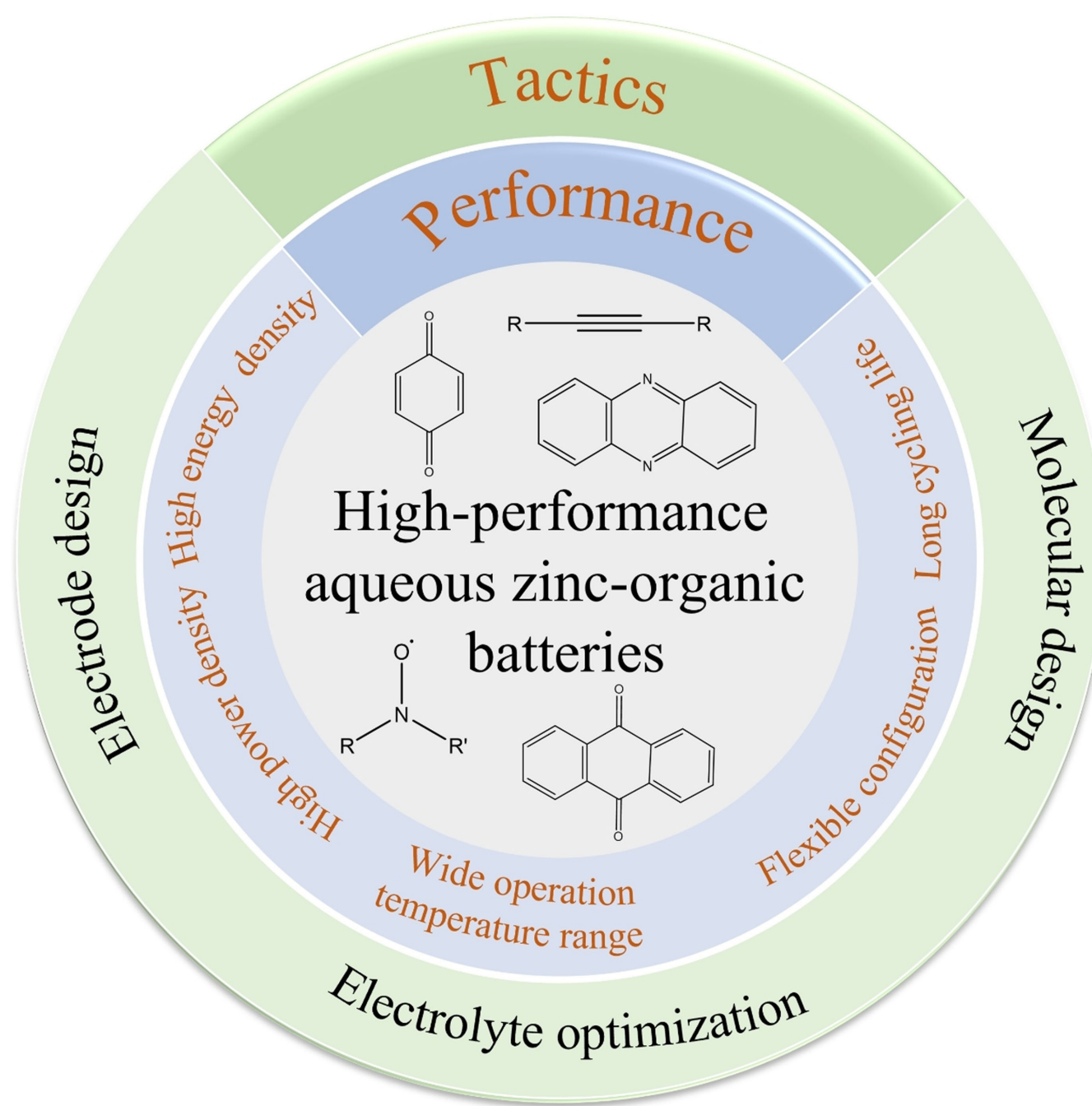


Special
Collection

Pathways towards High-Performance Aqueous Zinc-Organic Batteries

Wuhai Yang,^[a] Huijun Yang,^{*[b]} and Haoshen Zhou^{*[a, c]}

An increasingly growing market for electricity energy will be projected to double by 2050. Renewable energies, such as solar and wind, can be an effective way to address the challenge. However, the incompatibility between generation and consumption of electricity arises a considerable trouble when a huge amount of electricity coming from renewable sources finds no users, which could result in miserable failure of an aging grid. To secure the grid, the utilization and development of efficient energy storage technologies are highly demanded. Among the energy storage system (ESS), aqueous Zinc (Zn) batteries based organic material cathode have been regarded as an attractive candidate on account of its outstanding

superiorities compared with inorganic compounds. Although it has gained huge success in lab-scale, the long-standing challenges like inferior energy density, low power density, narrow operation temperature range and poor cycling life still restrict their practical application in aqueous Zn batteries (AZBs). In this minireview, we firstly provide a comprehensive insight into the different storage mechanisms that are proposed in varieties of organic cathodes. Based on the clear understanding on mechanisms, we further summarize the major progress and offer several promising research directions on promoting electrochemical performance of Zn-organic batteries.

1. Introduction

Among the existing battery technologies, rechargeable aqueous zinc (Zn) batteries attract major attention as a promising candidate in term of their outstanding superiorities, such as intrinsic safety, cost-effectiveness, and environmental friendliness.^[1–3] Currently, these conventional inorganic transition-metal oxides, such as manganese-based oxides, vanadium-based oxides, and Prussian blue analogs, are widely utilized as energy storage materials for aqueous Zn batteries (AZBs).^[4–8] Nevertheless, the lingering issues of inorganic compounds fail to satisfy the progress of large-scale and environmental-friendly energy storage systems (ESSs), because of the limited raw material resources and potential environmental pollution.^[4,9] In this context, organic compounds as cathode materials have received an extensive recognition from academia in view of their superior characteristics over inorganic materials.^[10–13] Firstly, the organic cathodes can be gained from biomass resources or mild artificial synthesis processes that are well established in the modern chemical industry. Therefore, it grants organic cathodes superiority of large-scale synthesis and the lower reaction temperature with minimal energy demands.^[11,14–16] In addition, organic compounds possess flexible structure designability, which allows the systematic adjustment of electrochemical performance for the desired ESS applications.^[16,17] More importantly, the high charge density

and sluggish diffusion of Zn^{2+} in the crystal lattice structure of inorganic cathodes hinders its electrochemical performance.^[18–20] By contrast, the molecules in organic materials stick together by weaker intermolecular interaction, i.e., van der Waals forces, which enables a lower Zn^{2+} diffusion barrier and a fast reaction kinetics.^[21] Finally, traditional inorganic materials are hardly to match the necessity of wearable electronics due to its heaviness and rigidity. By contrast, organic compounds could satisfy the surging needs of wearable power supply in daily life. Given these appealing points, organic materials show great potential for the next-generation AZBs toward practical applications.

However, the practical adoption of organic cathodes for AZBs still suffers from several problems and calls for in-depth analysis on ion storage mechanism. Arguably, one of the significant limitations is its low energy density compared with other configuration due to its low output voltage and poor capacity delivery.^[22–24] Besides, the intrinsic inferior ionic electronic conductivity of organic cathodes degrades its rate performance.^[17,25,26] Furthermore, organic cathodes generally undergo subsequent capacity fading as result of their high solubility in aqueous electrolyte,^[27] phase transformation,^[21] and the instability of intermediates.^[28] Recently, aiming at resolving the above-mentioned challenges, emerging approaches, such as molecular engineering, addition of conductive material, separator modification, optimization of electrolyte, polymerization and so on, have been put forward.^[29–32]

Although the widespread exploration of organic materials as cathode by battery community, there is still a huge gap between scientific findings in laboratory and target of practical requirements in terms of power density, energy density and battery cyclic lifespan. In this review, we herein systematically disclose the tactics toward improving the electrochemical performances (output voltage, specific capacity, cycling stability, operation temperature range and rate capability) of organic compounds for ongoing next-generation ESS research. It should be noted that the content of this contribution is not confined to progress in Zn-organic battery, also borrow some tactics that can apply in AZBs from other battery scenarios.

- [a] *W. Yang, Prof. H. Zhou
Graduate School of System and Information Engineering
University of Tsukuba
1-1-1, Tennoudai, Tsukuba 305-8573, Japan*
- [b] *Dr. H. Yang
Energy Technology Research Institute
National Institute of Advanced Industrial Science and Technology (AIST)
1-1-1, Umezono, Tsukuba 305-8568, Japan
E-mail: yang.hj@aist.go.jp*
- [c] *Prof. H. Zhou
Center of Energy Storage Materials & Technology, College of Engineering and Applied Sciences, Jiangsu Key Laboratory of Artificial Functional Materials, National Laboratory of Solid State Micro-structures, and Collaborative Innovation Center of Advanced Micro-structures
Nanjing University
Nanjing 210093, P. R. China
E-mail: hszhou@nju.edu.cn*

Special Collection
An invited contribution to a Special Collection dedicated to Aqueous Electrolyte Batteries

2. Working Principles

Considering that the reaction reversibility, redox potential, and specific capacity of organic materials electrode is determined by its storage mechanism,^[29] it is necessary to have an in-deep investigation of its charge storage mechanism. In generally, organic compounds can be classified into n-type, p-type, or bipolar-type materials on the basis of their electrochemically active groups (Table 1). The redox reactions for n-type organic compounds occur between the neutral state and the negatively discharged state. The reported n-type organics first undergo reduction and yield anion which coordinates with metal counterions to remain its electroneutral. Apart from Zn^{2+} , competitive H^+ insertion/dissertation behavior also has been observed in organic materials containing carbonyl group.^[33–35] In contrast to n-type organic materials, p-type cathodes lose an electron to form cation and combine with anions, such as Cl^- , ClO_4^- , SO_4^{2-} , $CF_3SO_3^-$ and BF_4^- , and so on, which are originated from the electrolyte.^[36] Bipolar-type compounds featured with properties of both p-type and n-type materials and can be first reduced or oxidized. The p-doping reaction happens at high voltage and the n-doping reaction occurs at low voltage, respectively.^[36] For a typical example, the half-oxidation state is present in PANI, i.e., doped ($-NH^+$) and undoped ($C=N-$) nitrogen. When PANI gains electron, $-NH^+$ is reduced to $-NH-$ and anions departure from the PANI. Otherwise, $C=N-$ will be reduced to electronegative nitrogen site ($C=N^-$) which coordinates with Zn^{2+} . During charge process, $C=N^-$ converts into $C=N-$ and Zn^{2+} will be removed from PANI. In the meantime, $-NH-$ is oxidized to $-NH^+$ which will coordinate with anion again.^[28]



Wuhai Yang is currently pursuing his Ph.D. degree in University of Tsukuba. He received his M.S. degree from the Qingdao University of Science and Technology in 2020. His current research focuses on the design of electrolytes for multivalent secondary batteries.



Huijun Yang is currently a JSPS postdoctoral fellow at the National Institute of Advanced Industrial Science and Technology (AIST) in Japan. He earned his B.S. (2016) and M.S. (2019) degrees at Shanghai Jiao Tong University (Supervisor: Prof. Jiulin Wang) and PhD degree (2021) at University of Tsukuba (Supervisor: Prof. Haoshen Zhou) in Japan, respectively. His research interests focus on the electrolyte and interphase of rechargeable batteries, including Li-ion, Li-sulfur, and Zn batteries.

3. High Energy Density

As following equations describes, the energy density of batteries is linked with the output voltage and specific capacity of cathode.^[38]

$$E_d = E \times Q$$

where E_d is the energy density, E is the working voltage, and Q is the specific capacity. For realization of high energy density, the battery with high output voltage and high capacity is urgently needed. The redox potential of organic electrode is highly associated with the lowest unoccupied molecule orbital (LUMO) energy. Function group is a crucial dictator for the working potentials of organic electrodes. The halogen atoms with strong electron-withdrawing ability, such as fluoro ($-F$), chloro ($-Cl$), bromo ($-Br$), can decrease the energy level of the lowest unoccupied molecular orbital (LUMO) and improve the working potentials of organic materials (Figure 1).^[9,37] Apart from halogen elements, other electron-withdrawing groups, such as cyano ($-CN$), trifluoromethyl ($-CF_3$), perfluorobutyl ($-C(CF_3)_3$), sulfonate ($-SO_3Na$), were also reported in lithium battery research areas to improve the redox potential of organic materials.^[9] Otherwise, the number of substituent groups also has a significant effect on working potential (Figure 1). However, additional functional group could result in increased molecular weight and its specific capacity will be sacrificed. Only balancing the relationship between active group and molecular weight, high energy density will be realized. Organic radicals are expected to have a higher working potential than other organic compounds due to its much lower LUMO energy level. Nishide and coworkers reported a radical polymer cathode, poly(2,2,6,6-tetramethylpiperidinyloxy-4-yl vinyl ether) (PTVE) which was consisted of hydrophilic poly(vinyl ether) backbone and 2,2,6,6-tetramethylpiperidine-1-oxyl (TEMPO) group.^[39] When it was paired with



Haoshen Zhou obtained his B.S. degree from Nanjing University in 1985 and received his PhD from the University of Tokyo in 1994. He is a professor in the College of Engineering and Applied Sciences, Nanjing University. His research interests include the synthesis of energy active materials and their applications in Li-ion batteries, Na-ion batteries, Li-redox flow batteries, metal-air batteries, and new type batteries/cells.

Table 1. Summary of properties of various organic materials.

Type	Materials	Advantages	Disadvantages
n-type	Carbonyl compounds, Imine compounds, Nitrile compounds, Organosulfur compounds, Azo compounds	High capacity, fast kinetics	High solubility, low conductivity
p-type	Nitronyl nitroxide, Organosulfur polymers, Triphenylamine derivatives	High voltage, fast kinetics	Low capacity
Bipolar type	Polyaniline, Polypyrrole, Poly(thiophene), Poly(3,4-ethylenedioxythiophene)	High conductivity	Low capacity

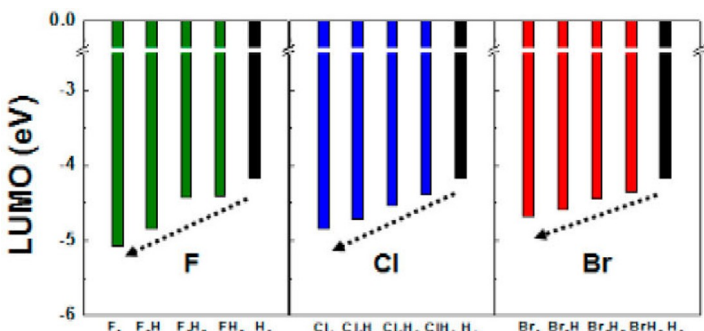


Figure 1. Comparison of LUMO energies of $C_6R_nO_2$ ($R=F, Cl, Br; n=0-4$) molecules using theoretical density functional theory (DFT) calculations. Reproduced with permission from Ref. [37]. Copyright (2015) American Chemical Society.

Zn anode, the battery showed a high working potential of 1.7 V. Moreover, the correlation between the working potentials of organic materials and relative position of active groups was discovered by Chen and his coworkers.^[27] The voltage of quinone with carbonyl groups in ortho-position (1,2-NQ and 9,10-PQ) were higher than those in para-position (1,4-NQ, 9,10-AQ). However, it should be noted that the quinone materials with carbonyls in para-position generally exhibited a higher capacity than those with carbonyls in ortho-position (Figure 2a), which is due to that the ortho carbonyls in quinones would cause larger steric hindrance for Zn^{2+} insertion.

The theoretical capacity (Q_{theo}) of electrode can be obtained as following equation:

$$Q_{\text{theo}} = \frac{nF}{3.6M_w}$$

where Q_{theo} represents the specific capacity of cathode (mAh g^{-1}), n is the number of transferred electrons, F is Faraday constant (Cmol^{-1}), and M_w represents molecular weight (g mol^{-1}).^[38] According to this equation, engineering organic molecules with more redox-active groups per molecular weight can be regard as an effective way to improve its theoretical capacity. Among a series of quinones, Chen and his coworkers found that calix[4]quinone (C4Q) with more active group per molecular weight displayed a highest capacity of 335 mAh g^{-1} and the Zn/C4Q battery configuration showed an energy density of 220 Wh kg^{-1} based the theoretical weight of cathode and anode. Another an organic material featured with a highly rich carbonyl group, pyrene-4,5,9,10-tetraone (PTO) which showed an excellent electrochemical performance (186.7 Wh kg^{-1} at a power density of 22.1 W kg^{-1}), was reported by Xia's group.^[41] Tao et al. proposed that a novel orthoquinone-based covalent organic framework (BT-PTO COF) was synthesized based on benzenetricarboxaldehyde (BT) node and

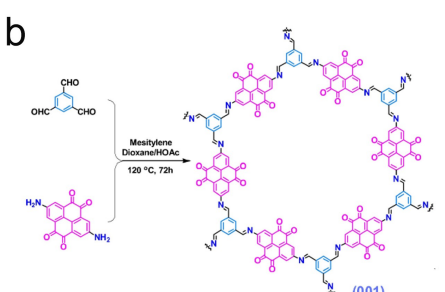
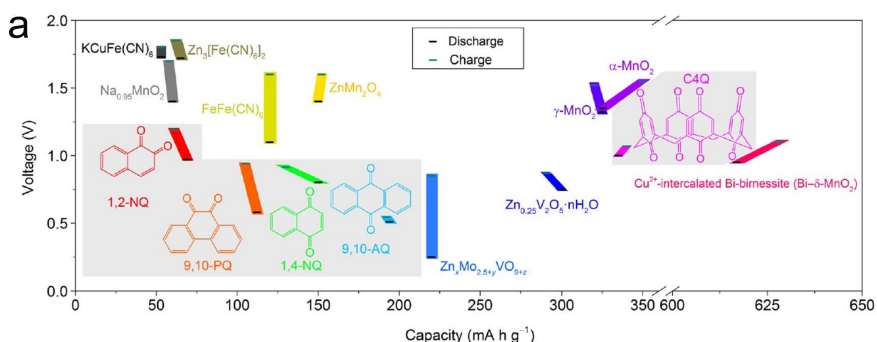


Figure 2. a) Specific capacities and discharge/charge voltages of different cathode materials. Reproduced with permission from Ref. [27]. Copyright (2018) American Association for the Advancement of Science. b) Synthesis procedure and the structure of the BT-PTO COF. Reproduced with permission from Ref. [40]. Copyright (2022) Wiley-VCH.

PTO (Figure 2b).^[40] It not only showed a specific power (184 kW kg⁻¹), but also a high energy density (92.4 Wh kg⁻¹) based on COF.

Furthermore, designing the efficient high-load electrodes is essential towards practical scenarios. However, the incomplete material utilization of active materials, i.e., only the outer layers of the active materials can be oxidized and reduced, brings about the unexpected lower capacity. Porous metal foams have been widely applied to provide electron pathway and enhance the electrochemical performance of batteries.^[44–46] Unfortunately, the metal substrates are easily corroded in aqueous solution. To solve the abovementioned problem, Si et al. showed that thin PANI layer was firstly coated onto the porous Ni foam by utilizing electrophoresis method and the resultant electrode was further covered by the PANI slurry under vacuum filtration to improve its load.^[47] Finally, the PANI cathode supported by Ni foam delivered a high specific capacity (183.28 mAh g⁻¹ at high current of 2.5 mA cm⁻²).

According to the electrochemical reaction process, the voltage (*E*) can be obtained as follow.

$$E = \frac{\Delta G}{nF},$$

where ΔG is the variation of Gibbs free energy, *n* is the number of transferred electrons, and *F* is Faraday constant. Li and coworkers revealed the influence of anion, such as CF_3SO_3^- , SO_4^{2-} , and ClO_4^- , on the electrochemical performance of the aqueous Zn/PTVE battery.^[42] From cyclic voltammetry (CV) characterizations and charge/discharge curves of Zn/PTVE battery in diverse electrolytes, the batteries using ZnSO_4 solution showed highest output voltage of 1.73 V (Figure 3a–f).

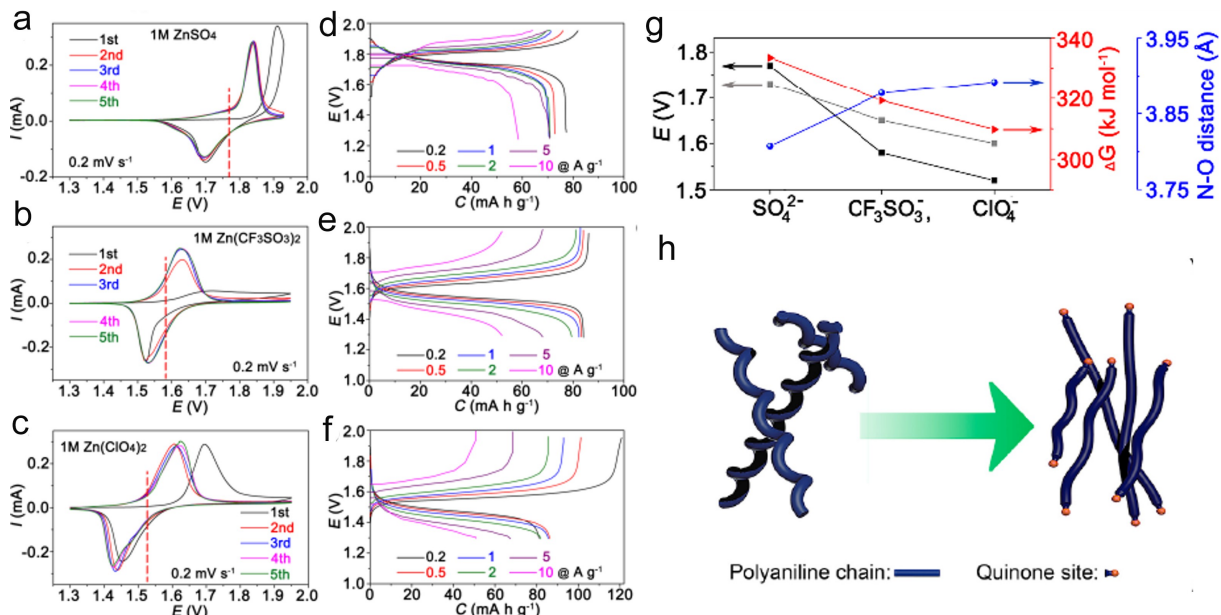


Figure 3. a–c) The results of CV test of Zn/PTVE with different aqueous electrolytes. d–f) Charge/discharge curves of Zn/PTVE with different aqueous electrolytes under different current densities. g) Experimental voltages (black), calculated voltages (gray), changes of Gibbs free energy (ΔG) of the battery reaction (red), and N–O distances (blue) for different solutions. Reproduced with permission from Ref. [42]. Copyright (2020) Wiley-VCH. h) Schematic illustration of the transformation of PANI from compact coil to expanded coil structure. Reproduced with permission from Ref. [43]. Copyright (2021) Elsevier.

According to DFT results, binding energy between PTVE unit (P^+) and SO_4^{2-} (1057.6 kJ mol⁻¹) was highest compared with $\text{P}^+ \bullet \text{CF}_3\text{SO}_3^-$ (521.7 kJ mol⁻¹) and $\text{P}^+ \bullet \text{ClO}_4^-$ (516.9 kJ mol⁻¹) and the largest ΔG value for the battery based on SO_4^{2-} electrolyte was realized (Figure 3g). Based on those results, it was concluded that regulating the operating voltages of battery by different anion in electrolyte is also highly feasible. What's more, similar phenomenon was also observed by Buda and coworkers.^[48]

High internal resistance of cathode will cause output voltage loss. Modifying the polymer chain conformation would be beneficial for increasing electronical conductivity. Sun and colleagues found that introduction of quinone-type active site onto PANI chain made transformation from a compact coil conformation to an expanded coil structure (Figure 3h), which improved its electrical conductivity and charge transfer of the polymer chain.^[43] Thanks to improved electrical conductivity, extra capacity and elevated voltage was realized.

4. High Power Density

The power density of rechargeable batteries is regarded as a prominent parameter to evaluate rechargeable batteries during charge-discharge processes. The power density can be obtained as follows:^[38]

$$P = E \times I$$

where *P* is the power, *E* is the output voltage, and *I* is the current. According to this equation, we can find that power density has a connection with current. High current performance demands fast mobility of electrons within electrode

during charge-discharge processes. However, the inferior electronic conductivity of organic materials limits its rate performance. Addition of conductive substrates, such as multi-walled carbon nanotubes (MWCNTs), graphene, carbon nanotubes (CNTs), and carbon fibers, has major impact on the battery performance. The polycatechol (PC) electrode combined graphene exhibited better rate capability (171 mAh g^{-1} at 10 C; retention of 74.4% after 3000 cycles at 2 C), which was due to the high electrical conductivity of graphene.^[49] Schubert and his colleagues showed that the composite of MWCNTs and poly(acetylene)-based polymer with 9,10-di(1,3-dithiol-2-ylidene)-9,10-dihydroanthracene moieties showed a high specific capacity of 111 mAh g^{-1} even at extremely high rate of 120 C (1 C = 133 mA g^{-1}).^[50] Owing to the unsatisfied electronic conductivity, mixture of CNTs and PEDOT was adopted to integrate the active PANI material.^[51] Even at a high current density of 10 A g^{-1} , a high capacity of 145 mAh g^{-1} was still maintained. The combination, graphite nanoplatelets and the PVA, was used as substrate for PANI, which brought a low internal resistance ($1.5 \Omega \text{ cm}^{-2}$) and a high power density (11.7 kW kg^{-1}).^[52] Moreover, additional binders which are widely used in electrodes, such as polyvinylidene fluoride (PVDF) and polytetrafluoroethylene (PTFE), is the one of reasons for the conductivity loss. Marcilla et al. showed that binder-free cathode composed of poly(catechol) redox copolymer and CNTs showed a remarkable capacities of 98 mAh g^{-1} at high rate of 450 C.^[53]

Organic cathodes are physically mixed with conductive materials, which could result in an inefficient conductive network. In situ synthesis of organic material on the conductive materials can further improve electrical conductivity of electrodes. Fatas and coworkers proposed that PANI was electro-deposited on a porous carbon rod.^[55] Lewis and colleagues showed that PANI was coated on the carbon fiber by electro-spinning and the battery maintained a capacity retention of 56% even at 18 C.^[56] PPY was also coated on the graphite and

stainless steel mesh substrates by the electro-polymerization method.^[57,58] Unfortunately, the battery still displayed fast capacity decay owing to relatively weak bonding between organic materials and substrates. Lee et al. proposed that breaking the C–C, C–N and C–H chemical bonds at the surface of carbon fiber by electroncyclotron-resonance plasma produced C radicals which combined reactive oxygen species (O^+ , O_2^+ , O_2^+ , and O_2^{2+}), which form oxygen functional groups ($-\text{OH}$, $-\text{COOH}$, and $-\text{C=O}$).^[54] The oxygen functional groups interacted with PANI to form N–O and N–H bonds (Figure 4), leading to an improved adhesion between PANI and carbon fibers. Liu et al. proposed that PDA was grafted on dispersed CNT by polymerization of dopamine in a basic aqueous solution.^[59] Thanks to its bio-adhesion effect, PDA adhered to the conductive CNTs strongly, contributing to high rate capability.

Cai et al. showed a Zn/electrospun poly(5-cyanoindole) fibers battery system. With the average fiber diameter decreasing, the electrical conductivity of poly(5-cyanoindole) fibers increased, which guaranteed Zn/poly(5-cyanoindole) fibers battery with discharge capacity of the 61 Ah kg^{-1} at 10 C.^[60] On the other hand, increasing specific surface area of cathode will greatly favor high rate performance. Lewis and coworkers reported that the PANI/CF cathode with high surface area could operated at 600 C, which corresponded to charge and discharge times of 6 s.

Restricted by Zn^{2+} insertion/extraction chemistry, Zn-ion batteries hardly meet the ever-increasing demand for high power rate in specific markets.^[61] In this context, utilizing H^+ with small ionic radius and low relative atomic mass as charge carriers gives solution to this hurdle. Niu et al. reported the diquinoxalino [2,3-a:2',3'-c] phenazine (HATN) synthesized by a simple dehydration condensation reaction.^[33] Solid-state NMR proofed that it experienced a H^+ insertion/deinsertion behavior in a ZnSO_4 electrolyte. Tao et al. reported that orthoquinone-based covalent organic framework (BT-PTO COF) cathode

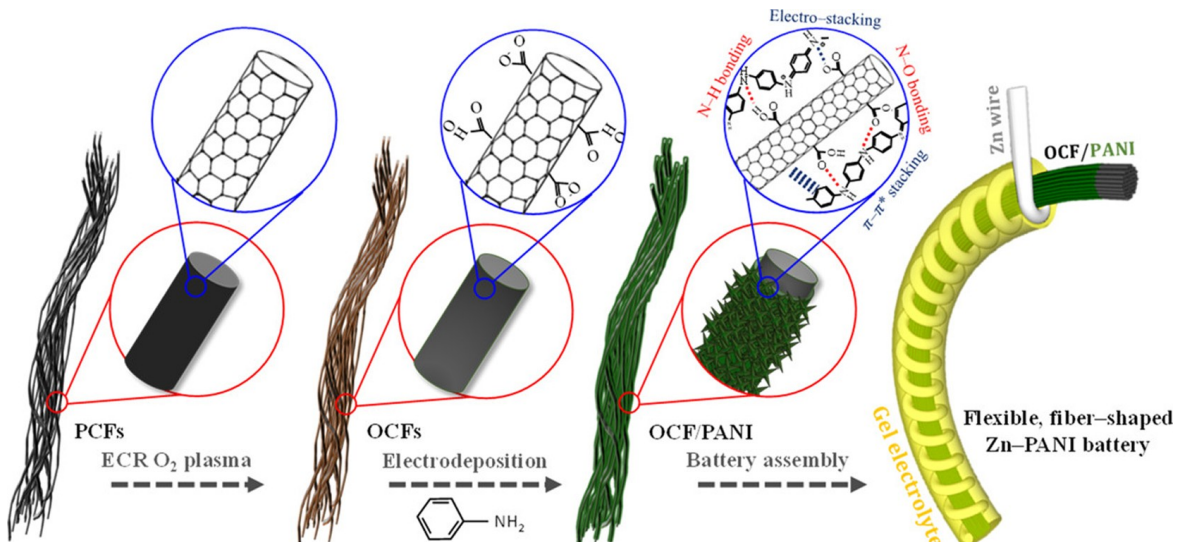


Figure 4. Schematic diagram of preparation of OCF/PANI cathode. Reproduced with permission from Ref. [54]. Copyright (2020) American Chemical Society.

displayed fast kinetic behavior.^[40] When the current was stepped up by 170 times (0.05 to 85 A g⁻¹), the value of capacity of BT-PTO COF fell from 220 mAh g⁻¹ to 170 mAh g⁻¹ only. Revealed by kinetic analyses, the evolution of insertion route from the H⁺, Zn²⁺ co-insertion to more H⁺ insertion routes at high current density occurred. The dominated H⁺ de/intercalation gave BT-PTO COF an ultra-fast kinetic behavior. Sun et al. showed tetraamino-p-benzoquinone (TABQ) and its amino groups promoted the redox of carbonyl group.^[35] As proved by EIS measurements, the value of activation energy E_a for charge transfer processes was only 288 meV with help of amino groups. Apart from that, a Grotthuss-type mechanism through the hydrogen bonding network between the amino and carbonyl groups realized facile proton conduction among TABQ molecules. The galvanostatic intermittent titration technique (GITT) showed that activation energy for ion diffusion was 181 meV. In addition, the co-insertion of H₂O molecules with Zn²⁺ can be also helpful in realizing high rate. Stoddart and his coworkers found that insertion of hydrated Zn²⁺ ions in the phenanthrenequinone-based macrocycle (PQ-Δ) cathode could decrease the desolvation energy penalty.^[62] When the current density increased from 30 mA g⁻¹ to 150 mA g⁻¹, the capacity loss was only 6.7% of original capacity. The rate performance is also associated with electrolyte composition, such as solvent and salt.^[63,64] The increased viscosity and lower ionic conductivity of electrolyte will restrict mass transport and lower the rate capability of battery.

5. Long Cycle Life

The redox activity PANI strongly depends on pH of electrolyte, and it requires high concentration of H⁺ to realize efficient redox processes. However, Zn metal anode remains terribly unstable in high acidic environment. A series of pH-sensitive functional group, such as -SO₃H, -COOH and -OH, was introduced as a proton reservoir for PANI to retain high local H⁺ concentration in its vicinity.^[65,66] Chen et al. proposed a sulfo self-doped PANI electrode obtained by the electrochemical copolymerization of aniline and metanilic acid to maintain the H⁺ concentration near the PANI cathode. A new copolymer, poly(anilineco-m-aminophenol), was synthesized and studied by Mu et al.^[66] The hydroxyls in the copolymer chain could not only regulated the pH values nearby the cathode, but also can be oxidized and reduced reversibly to improve the specific capacity. Also, another redox-active N-methylthionine unit was introduced into polyaniline chain via electrochemical copolymerization. The phenothiazine ring can be reversibly electrochemically oxidized and reduced even in the basic electrolytes.^[67,68] However, the relatively cumbersome synthesis procedures reduce its practicality. A method, blending PANI with polystyrene sulfonate (PSS) which contained -SO₃H group, was proposed by Huang and coworkers, which enabled easiness in electrode manufacturing handling.^[51] Li et al. showed another approach by introducing the graphene oxide (GO) sheets as a particular dopant. The GO component containing a plethora of oxygen-containing functional groups also could

supply local proton reservoir for PANI.^[69] For PANI, the instability of water is another cause of its inferior performance in aqueous electrolyte. The oxidized state of PANI would react with the water molecular in aqueous solution, leading to the serious capacity loss.^[28] Yang and coworkers prepared the PANI-[Fe(CN)₆]⁴⁻ electrode on the surface of carbon cloth (CC) via a uncomplicated and cost-effective strategy.^[70] The strong interaction between [Fe(CN)₆]⁴⁻ and PANI weaken the interaction between water and PANI (Figure 5a) and suppressed the decomposition of water was suppressed, which contributed the higher specific capacity retention rate (71%) of CC-PANI-FeCN in ZnSO₄ aqueous solution compared with CC-PANI (17%). In addition, the specific capacity of CC-PANI-FeCN without binder was only reduced by ~23.3% when current density increased from 1 to 5 A g⁻¹. The nanosized effect also has a significant effect on redox activity of cathode. Mu et al. showed that poly (Ani-co-5-ASA) nanowires with different sizes was obtained using the electrochemical way by controlling the applied potentials.^[71] They found that the redox activity of poly (Ani-co-5-ASA) nanowires with smaller diameters was higher than that of nanowires with bigger diameter.

Shao et al. substituted the O in C—O—C bonds of 1,4,5,8-naphthalenetetracarboxylic dianhydride (NTCDA) by N to synthesize 1,4,5,8-naphthalene dimide (NTCDI) (Figure 5b).^[72] During their investigation, they found that NTCDA suffered from fast capacity fading, which was attributed to that the original structure of NTCDA was destroyed by the trapping of Zn²⁺. The higher charge density of Zn²⁺ resulted in strong interaction between Zn²⁺ and NTCDA and incomplete utilization of NTCDA. The EIS test showed a high impedance difference of NTCDA, indicating the high electronic resistance and low charge transfer rate of NTCDA. In contrast to that, there was no variation on the structure of NTCDI. Finally, it displayed a highly capacity (240 mAh g⁻¹ at 0.1 A g⁻¹) and a long cycle stability (over 2000 cycles with a capacity retention of 73.7%). It is well known that organic molecules with high symmetry possess low solubilities in aqueous solutions.^[73] Sun et al. demonstrated that tetraamino-p-benzoquinone (TABQ) with four amino groups was used as the cathode material for AZBs.^[35] Contributed by its highly symmetry structure, TABQ displayed stable capacity retention for over 1000 cycles and high value of coulombic efficiencies (100%). Stabilizing cathode through the construction of intermolecular S—S interactions between the heterocyclic thioether group (C—S—C) by oxidizing the dithioether moiety was also effective method to suppress dissolution of cathode (Figure 5c).^[74] A sulfur heterocyclic quinone dibenzob[b,i]thianthrene-5,7,12,14-tetraone (DTT) reported by Wang and coworkers was utilized as the cathode in AZBs.^[75] During their investigation, they found that H⁺ and Zn²⁺ co-reacted with carbonyl group of DTT. The results of DFT showed that the main discharged product of DTT was DTT₂(H⁺)₄(Zn²⁺) configuration (Figure 6). Two adjacent DTT molecules was connected by Zn²⁺, which suppressed the dissolution of DTT. This guaranteed that Zn/DTT cell showed a stable cycling life (23,000 cycles) and high capacity retention (83.8%). Otherwise, extending the π-conjugated system are reported to strengthen the π-π intermolecular interactions,

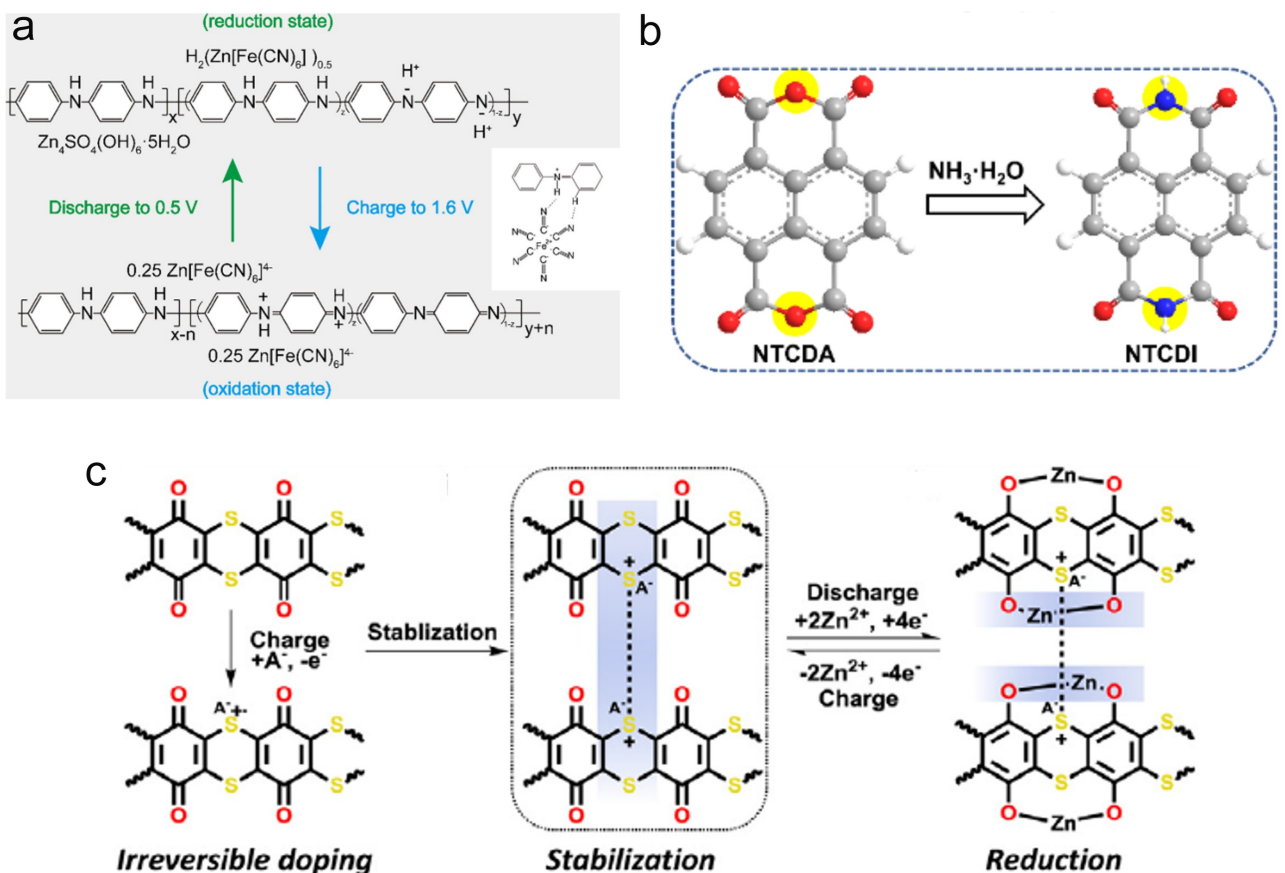


Figure 5. a) The proposed reaction mechanism of CC-PANI-FeCN during charge/discharge process. Inset: schematic illustration of the interaction between $[\text{Fe}(\text{CN})_6]^{4-}$ and PANI. Reproduced with permission from Ref. [70]. Copyright (2020) Elsevier. b) The synthesis procedure of NTCDI. Reproduced with permission from Ref. [72]. Copyright (2019) Wiley-VCH. c) The variation of structure of PDB after the initial charge. Reproduced with permission from Ref. [74]. Copyright (2020) Elsevier.

which decreased the solubility of organic molecules and enhanced the cyclability of organic cathodes.^[76] However, this strategy has not been implemented in aqueous Zn electrolyte. The polymerization is also proved as an effective way to mitigate the dissolution issue of small organic carbonyl compounds. Chen et al. showed that the polymer, poly(benzoquinonyl sulfide) (PBQS), was used as cathode and it delivered a capacity retention of 86% after 50 cycles at 0.2 C.^[77]

The discharge product of quinone electrodes suffers from severe dissolution because of free water in aqueous solution. Nafion membrane with full of sulfonic acid was introduced as a separator.^[27] Thanks to the negatively charged groups (e.g., SO_3^{2-}) of the membrane, the free crossing of discharge product of cathode was effectively blocked. In addition, another practice regarding electrolyte renovation is utilizing high concentration electrolytes. The interaction between solvent and ion is reinforced as the increase of salt concentration.^[63,78-80] Therefore, the confined state of major water molecular considerably mitigated its solvating capability (Figure 7a).^[81-84] Benefiting from this character, cathode dissolution in high-concentrated electrolyte could be inhibited.^[85,86] Otherwise, utilizing neutral ligand with hydrogen acceptors and donors also can decrease free-state water molecules (Figure 7b).^[87-89] Cui et. al. proposed a hydrated eutectic electrolytes (succinoni-

trile/ $\text{Zn}(\text{ClO}_4)_2 \cdot 6\text{H}_2\text{O}$) with limited water to suppress the dissolution of a quinone-based polymer cathode, poly(2,3-dithieno-1,4-benzoquinone) (PDB).^[90] Because of the reduced cathode dissolution, the battery configuration favored battery cycling (a low capacity decay rate of 14% and long cycling life of 3,500 cycles).

The separation between cathode and conductive carbon framework caused by a phase transfer mechanism is another cause for bad electrochemical rechargeability. Kundu et al. showed that tetrachloro-1,4-benzoquinone (p-chloranil) reacted with water and formed soluble quinols between cathode and electrolyte.^[21] However soluble quinols are not found in the electrolyte. The quinol molecules underwent a metathesis with Zn^{2+} and formed a Zn-p-chloranil crystal (Figure 8). This structural transformation resulted in disconnection between cathode and conductive carbon framework. The conductive carbon, CMK-3 was utilized to confining p-chloranil in its mesoporous nanochannels by nanoconfinement strategy, which guaranteed compact contact of cathode with the conductive carbon and improved cycling life. Also, a very high energy efficiency of ~95% was obtained due to the low voltage polarization between p-chloranil and Zn-p-chloranil.

Zn anode suffers from massive by-product formation and accumulation which arises from uncontrollable water-related

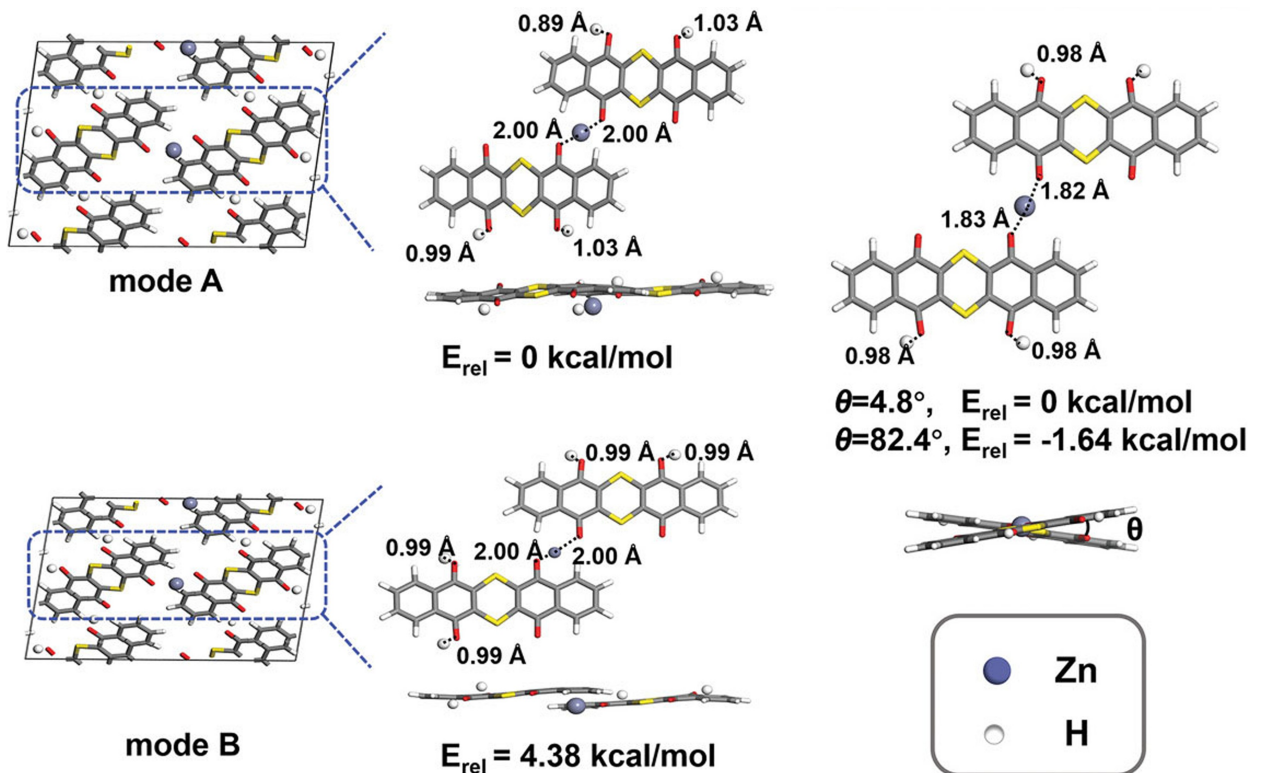


Figure 6. The geometries and relative energies (E_{rel}) of $\text{DTT}_2(\text{H}^+)_4(\text{Zn}^{2+})$ optimized by DFT utilizing both periodic boundary condition model and cluster model. Reproduced with permission from Ref. [75]. Copyright (2020) Wiley-VCH.

parasite reactions at the vicinity of electrolyte/anode interface.^[91–93] Replacing the Zn metal with other active materials whose reduction potential are higher than Zn^{2+}/Zn as anode can directly solve the problem in rechargeable AZBs. Liang et al. showed that 9,10-anthraquinone (AQ) was applied as anode material and the full battery, AQ/ZnMn₂O₄, displayed the capacity retention of 94.4% even after 500 cycles.^[94]

6. Flexible Configuration and Wide Operation Temperature Range

Batteries with ability to endure large tensile offer many application possibilities. However, conventional inorganic materials were easily fragile under the external force. Niu et al. proposed a flexible all-in-one ZIBs consisting of reduced graphene oxide/polyaniline (rGO/PANI) and it shows excellent physical flexibility and superior integrity.^[95] Energy storage devices stacked from two electrodes and a separator also suffer from the possible delamination under deformed states, which could deteriorate its electrochemical performance. An integrated and flexible Zn battery was made by electrodeposition of polyaniline and Zn anode on a filter paper coated with current collectors.^[96] The battery configuration showed no delamination and capacity loss after bending, folding, and twisting.^[41] Xia et al. proposed that the belt-shaped Zn/PTO battery showed a robust mechanical durability and remarkable

flexibility. Even after the flat battery bent at a different angle, there was almost no discernible capacity loss (Figure 9a and 9b). A highly compressible ZIBs composed of polyaniline (PANI) and single-walled carbon nanotubes (SWCNTs) coated sponge was reported by Niu and his coworkers (Figure 9c).^[97] The battery displayed excellent capacity retentions of 90.7% and nearly 100% at 0% and 60% strains, respectively, when it was continuously compressed for 1000 times.

Wide operational temperature ranges for Zn-organic batteries are also in urgent demand.^[98,99] The use of concentrated electrolyte is an effective way to widen operational temperature ranges of electrolyte. Marcilla et al. showed that 4 M $\text{Zn}(\text{TFSI})_2$ aqueous electrolyte demonstrated a more negative temperature.^[53] Otherwise, another Zn slat containing fluorine element, $\text{Zn}(\text{BF}_4)_2$, was reported by Tao et al. and an ultralow freezing point, -122°C , was realized.^[100] Chen et al. modulated electrolyte structure by optimizing the concentration of ZnCl_2 and a low freezing point (-114°C) of electrolyte was realized.^[101] Finally, the aqueous electrolyte guaranteed that the full batteries, PANI/Zn, could operate smoothly in a wide temperature range from -90°C to $+60^\circ\text{C}$. In addition to utilizing concentrated electrolyte, another practice regarding electrolyte renovation is that using organic solvents to suppress the freeze of aqueous electrolyte. Recently, Cui et al. showed a hydrated eutectic electrolyte composed of succinonitrile (SN) and $\text{Zn}(\text{ClO}_4)_2 \cdot 6\text{H}_2\text{O}$.^[90] Thanks to the rich intermolecular interactions among water, SN and Zn salt, low freezing point (-90°C) was obtained. Also, Zn/Zn symmetric cell under

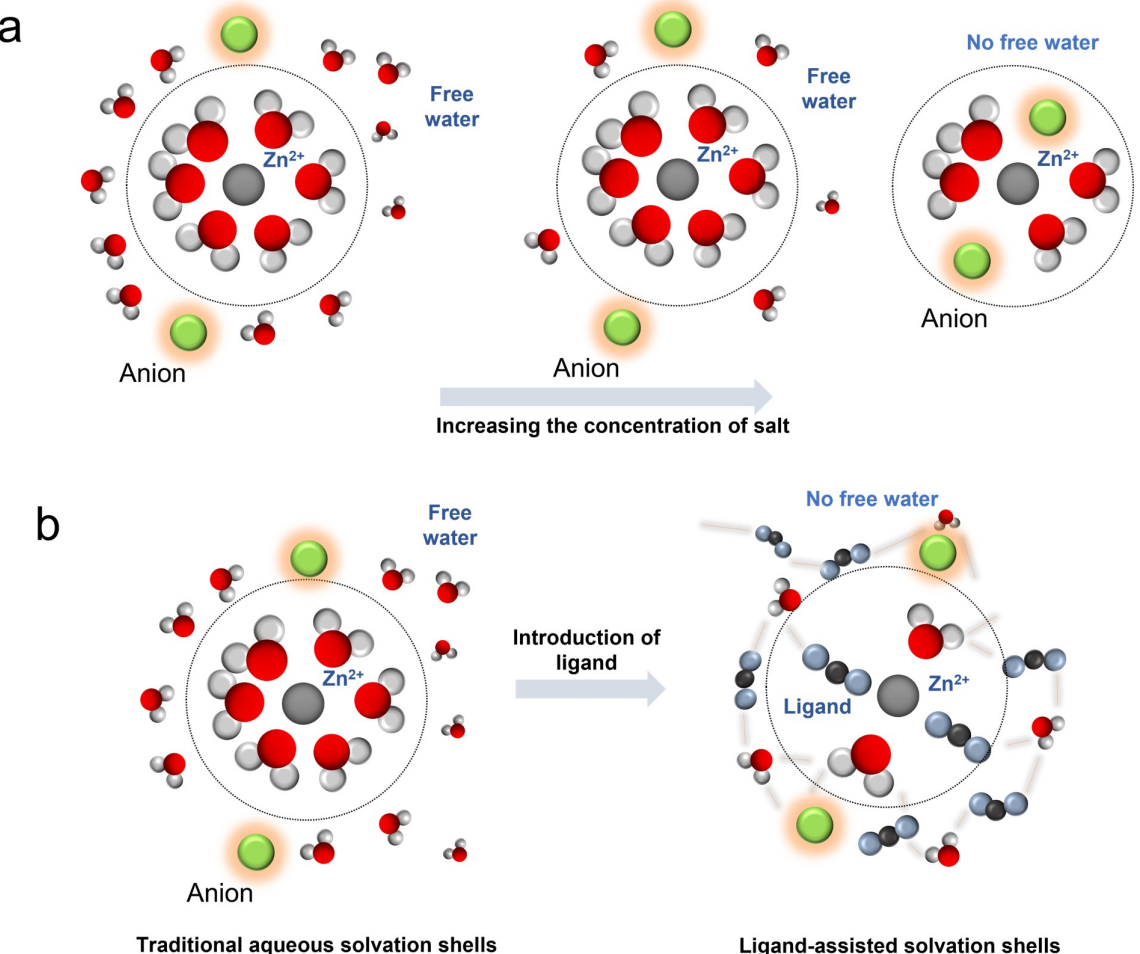


Figure 7. Evolution of state of water in a) concentrated electrolytes and b) hybrid electrolytes.

galvanostatic conditions could work well even at high temperature (90 °C). Guo et al. reported that triethyl phosphate (TEP) with a high Gutmann donor number was utilized as cosolvent to regulate the structure of electrolyte and a temperature range of –20 °C to 20 °C was realized.^[87] Otherwise, other solvent such as methanol and ethylene glycol can help battery work well even under harsh environments.^[102,103]

7. Conclusion and Perspective

Zn batteries based on organic cathodes have the potential to satisfy the future demands of large-scale energy storage because of its relatively high abundance of elements, low-cost, ease of manufacture, safety, and environmentally benign characters. The reported performance of different kinds of representative organic cathodes in Zn batteries are summarized in Table 2. However, they face a series of endogenous challenges, such as lower output voltage, low capacity, inferior battery longevity, and bad rate performance and various methods to solve the abovementioned problems was summarized (Table 3).

High discharge potential and high specific capacity would be achieved in the following: 1) Introduction of electron-withdrawing groups and increasing its amounts can improve the voltage effectively. Unfortunately, introducing too many groups will bring about the increase of molecular weight and specific capacity will be sacrificed correspondingly. Therefore, it is crucial to evaluate the trade-off between molecular weight and amounts of group. 2) Improving working potentials of battery can be achieved by reducing the internal resistance. 3) Engineering organic materials with more redox-active sites per molecular weight could boost the specific capacity. 4) The relative position between active group not only determined the voltage but also capacity. 5) Different anion species in solution contribute different reaction energy levels, resulting in different operating voltages of battery.

The rate performance of battery is highly associated with the conductivity of electrode. The hybridization of organic compounds with conductive substrates can bring about enhanced electronic conductivity. Intensifying the interaction between cathode and conductive can obtain additional enhancement of conductivity. Otherwise, replacing Zn^{2+} by H^+ as charge carrier would open new opportunities to construct a high-rate performance AZBs.

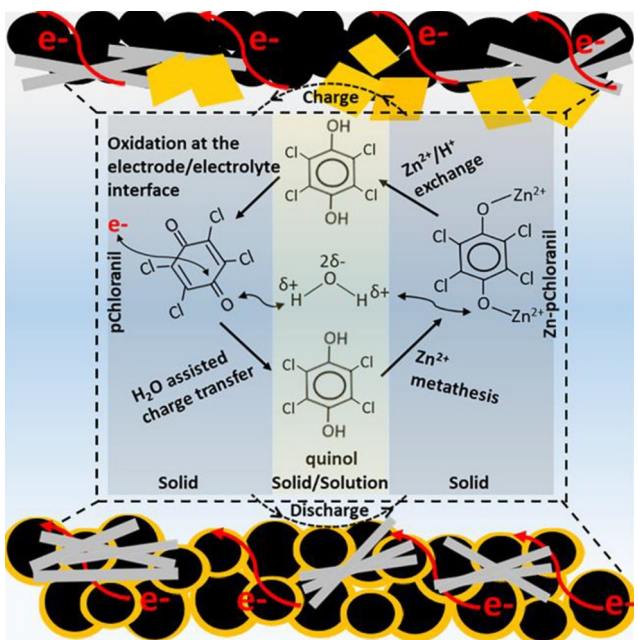


Figure 8. Schematic illustration phase transfer mechanism (discharged Zn-p-chloranil in gray and charged p-chloranil in yellow). Reproduced with permission from Ref. [21]. Copyright (2018) American Chemical Society.

For PANI cathode, introduction of H⁺ reservoir group and reducing the interaction between water and PANI to suppress the decomposition of water will be helpful in achieving long cycling life. Organic cathode suffers from dissolution because of high solvating ability of free water in aqueous solution, which results in serious capacity loss. Concentrated electrolyte or hybrid electrolytes could reduce the free water and suppress cathode dissolution. Regulating the molecule structure, intensifying the interaction between organic molecules, separator modification, and polymerization can be regarded as effective methods to suppress the dissolution of cathode. Utilizing conductive carbon with mesoporous nanochannels could suppress separation between cathode and conductive material. To avoid issues of Zn anode passivation/cell failure, organic material can replace Zn metal as anode.

The realization of batteries with ability to endure large tensile requires highly flexible electrodes. However, inorganic materials suffer from fragility under the force. Organic cathodes will be conducive to developing next-generation flexible and wearable electronics due to its flexibility. To widen operational temperature ranges of Zn-organic batteries, optimizing the electrolyte composition will be an effective solution.

In conclusion, the factor that determined the electrochemical performance of Zn-organic battery was compiled. We

Table 2. Summary of the electrochemical performance of representative organic electrode materials.

Materials	Voltage [V]	Capacity [mAh g ⁻¹]	Cycling Life [No. of cycles]	Rate Capability	Ref.
PTVE	1.7 V	131 mAh g ⁻¹	Over 500 cycles	1200 C	[39]
1,2-NQ	~1.0 V	~70 mAh g ⁻¹	5 cycles	\	[27]
9,10-PQ	~0.95 V, ~0.6 V	~110 mAh g ⁻¹	5 cycles	\	[27]
1,4-NQ	~0.8 V	~150 mAh g ⁻¹	5 cycles	\	[27]
9,10-AQ	~0.5 V	~200 mAh g ⁻¹	5 cycles	\	[27]
C4Q	1.0 V	335 mAh g ⁻¹	1000 cycles	1000 mA g ⁻¹	[27]
PTO	~0.8 V	336 mAh g ⁻¹	1000 cycles	20 Ag ⁻¹	[41]
BT-PTO	~0.85 V	221 mAh g ⁻¹	10000 cycles	1785 C (500 Ag ⁻¹)	[40]
COF	/	/	/	/	/
PC	/	355 mAh g ⁻¹	3000 cycles	10 C	[49]
PANI	~1.10 V	200 mAh g ⁻¹	3000 cycles	5 Ag ⁻¹	[28]
NTCDA	~0.6 V, ~0.4 V	170 mAh g ⁻¹	5 cycles	2 Ag ⁻¹	[72]
NTCDI	~0.5 V	240 mAh g ⁻¹	2000 cycles	2 Ag ⁻¹	[72]
HATN	~0.5 V	405 mAh g ⁻¹	5000 cycles	20 Ag ⁻¹	[33]
TABQ	~0.8 V	303 mAh g ⁻¹	1000 cycles	5 Ag ⁻¹	[35]
DTT	~0.8 V	210.9 mAh g ⁻¹	23000 cycles	2 Ag ⁻¹	[75]
PBQS	0.95 V	203 mAh g ⁻¹	50 cycles	5 C	[77]
PDB	0.9 V	100 mAh g ⁻¹	3500 cycles	1.2 C	[90]
p-chloranil	1.1	200 mAh g ⁻¹	200 cycles	1 C	[21]

Table 3. Summary of strategies to improve the performance of the battery.

Performance	Strategies
High energy density	Molecular design like introduction of electron-withdrawing group, position/number of groups, increasing number of the active group and so on Improving the material utilization of active materials with help of porous metal foams Electrolyte modification
High power density	Electrode design such as introduction of conductive substrates, intensifying the interaction between organic material and conductive substrates, increasing specific surface area of cathode, improving the intrinsic electronic conductivity of cathode and so on Optimizing the coordination action
Long cycling life	Molecular design like introduction of functional group, regulating the structure of organic molecule and so on Electrolyte modification Electrode design
Flexible configuration	Electrode design
Wide operation temperature range	Electrolyte modification

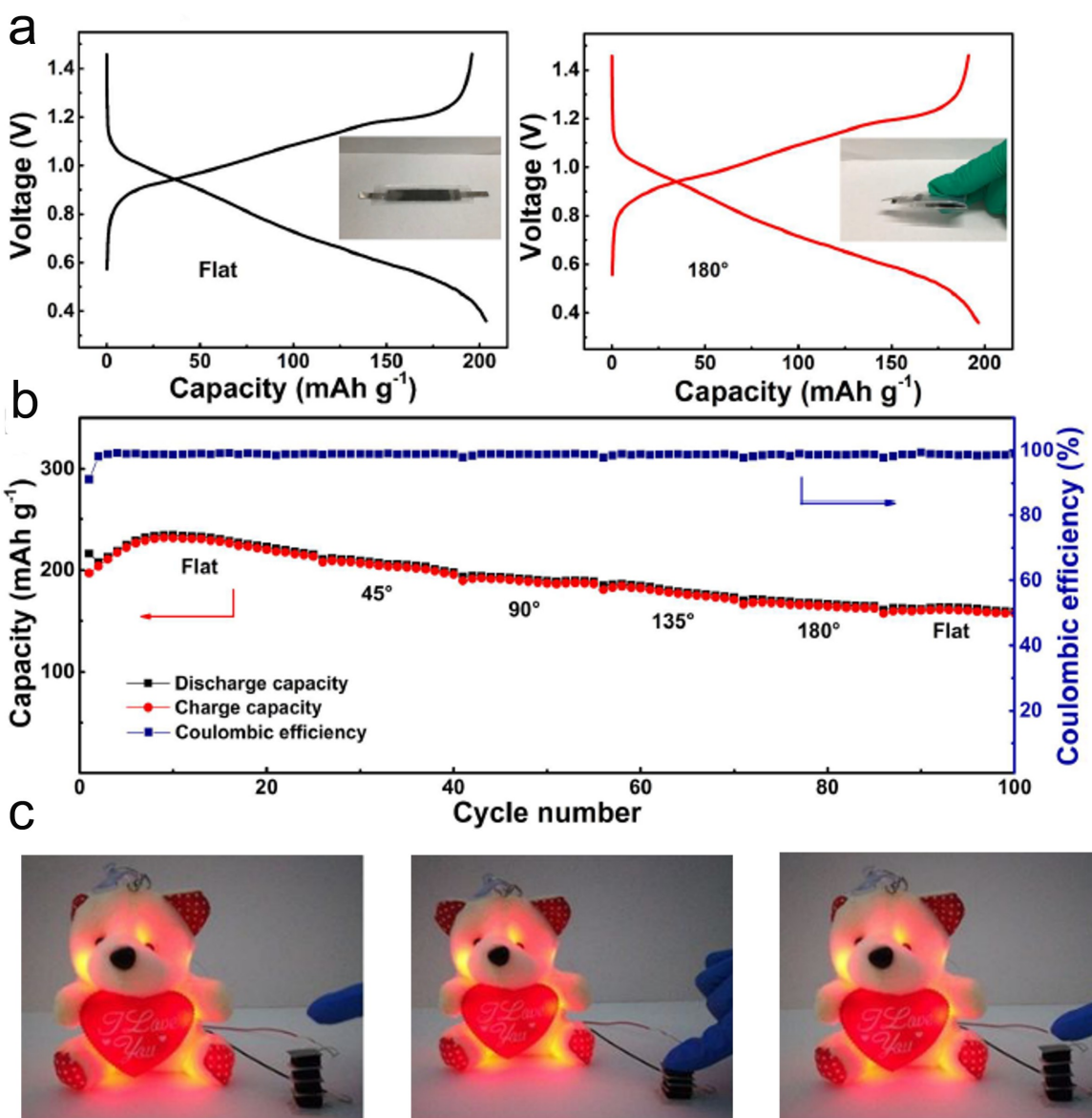


Figure 9. a) The discharge/charge profiles of the Zn/PTO battery at flat (left) and folded state (180°) (right) for 100 times. b) Cycle stability of Zn/PTO battery at different bending states. Reproduced with permission from Ref. [41]. Copyright (2018) Wiley-VCH. c) The optical picture of LEDs lighted by integrated Zn battery at the compressing and recovering state. Reproduced with permission from Ref. [97]. Copyright (2019) Royal Society of Chemistry.

hope this review will give reader insights in designing high performance Zn-organic battery.

Keywords: aqueous Zn batteries · electrochemical performance · energy storage mechanism · organic cathode

Acknowledgements

W.Y. acknowledges scholarships from China Scholarship Council (CSC).

Conflict of Interest

The authors declare no conflict of interest.

- [1] L. Ma, M. A. Schroeder, O. Borodin, T. P. Pollard, M. S. Ding, C. Wang, K. Xu, *Nat. Energy* **2020**, *5*, 743.
- [2] J. F. Parker, C. N. Chervin, I. R. Pala, M. Machler, M. F. Burz, J. W. Long, D. R. Rolison, *Science* **2017**, *356*, 415.
- [3] H. Yang, Y. Qiao, Z. Chang, H. Deng, X. Zhu, R. Zhu, Z. Xiong, P. He, H. Zhou, *Adv. Mater.* **2021**, *33*, e2102415.
- [4] M. Song, H. Tan, D. Chao, H. J. Fan, *Adv. Funct. Mater.* **2018**, *28*, 1802564.
- [5] C. Xu, B. Li, H. Du, F. Kang, *Angew. Chem. Int. Ed.* **2012**, *51*, 933.
- [6] D. Kundu, B. D. Adams, V. Duffort, S. H. Vajargah, L. F. Nazar, *Nat. Energy* **2016**, *1*, 16119.
- [7] W. Sun, F. Wang, S. Hou, C. Yang, X. Fan, Z. Ma, T. Gao, F. Han, R. Hu, M. Zhu, C. Wang, *J. Am. Chem. Soc.* **2017**, *139*, 9775.

- [8] H. Pan, Y. Shao, P. Yan, Y. Cheng, K. S. Han, Z. Nie, C. Wang, J. Yang, X. Li, P. Bhattacharya, K. T. Mueller, J. Liu, *Nat. Energy* **2016**, *1*, 16039.
- [9] T. Yokooji, H. Matsubara, M. Satoh, *J. Mater. Chem. A* **2014**, *2*, 19347.
- [10] H. Dong, O. Tutusaus, Y. Liang, Y. Zhang, Z. Lebens-Higgins, W. Yang, R. Mohtadi, Y. Yao, *Nat. Energy* **2020**, *5*, 1043.
- [11] Y. Lu, J. Chen, *Nat. Chem. Rev.* **2020**, *4*, 127.
- [12] A. Jouhara, N. Dupre, A. C. Gaillot, D. Guyomard, F. Dolhem, P. Poizot, *Nat. Commun.* **2018**, *9*, 4401.
- [13] Z. Song, Y. Qian, X. Liu, T. Zhang, Y. Zhu, H. Yu, M. Otani, H. Zhou, *Energy Environ. Sci.* **2014**, *7*, 4077.
- [14] T. B. Schon, B. T. McAllister, P. F. Li, D. S. Seferos, *Chem. Soc. Rev.* **2016**, *45*, 6345.
- [15] B. Häupler, A. Wild, U. S. Schubert, *Adv. Energy Mater.* **2015**, *5*, 1402034.
- [16] R. Rajagopalan, Y. Tang, C. Jia, X. Ji, H. Wang, *Energy Environ. Sci.* **2020**, *13*, 1568.
- [17] S. Lee, G. Kwon, K. Ku, K. Yoon, S. K. Jung, H. D. Lim, K. Kang, *Adv. Mater.* **2018**, *30*, e1704682.
- [18] N. Zhang, Y. Dong, M. Jia, X. Bian, Y. Wang, M. Qiu, J. Xu, Y. Liu, L. Jiao, F. Cheng, *ACS Energy Lett.* **2018**, *3*, 1366.
- [19] D. Kundu, S. Hosseini Vajargah, L. Wan, B. Adams, D. Prendergast, L. F. Nazar, *Energy Environ. Sci.* **2018**, *11*, 881.
- [20] F. Wang, E. Hu, W. Sun, T. Gao, X. Ji, X. Fan, F. Han, X.-Q. Yang, K. Xu, C. Wang, *Energy Environ. Sci.* **2018**, *11*, 3168.
- [21] D. Kundu, P. Oberholzer, C. Glaros, A. Bouzid, E. Tervoort, A. Pasquarello, M. Niederberger, *Chem. Mater.* **2018**, *30*, 3874.
- [22] X. Qiu, N. Wang, Z. Wang, F. Wang, Y. Wang, *Angew. Chem. Int. Ed.* **2021**, *60*, 9610.
- [23] Y. Zhao, Y. Wang, Z. Zhao, J. Zhao, T. Xin, N. Wang, J. Liu, *Energy Storage Mater.* **2020**, *28*, 64.
- [24] Y. Liang, H. Dong, D. Aurbach, Y. Yao, *Nat. Energy* **2020**, *5*, 646.
- [25] T. Janoschka, M. D. Hager, U. S. Schubert, *Adv. Mater.* **2012**, *24*, 6397.
- [26] D. J. Kim, D.-J. Yoo, M. T. Otley, A. Prokofjevs, C. Pezzato, M. Owczarek, S. J. Lee, J. W. Choi, J. F. Stoddart, *Nat. Energy* **2018**, *4*, 51.
- [27] Q. Zhao, W. Huang, Z. Luo, L. Liu, Y. Lu, Y. Li, L. Li, J. Hu, H. Ma, J. Chen, *Sci. Adv.* **2018**, *4*, eaao1761.
- [28] F. Wan, L. Zhang, X. Wang, S. Bi, Z. Niu, J. Chen, *Adv. Funct. Mater.* **2018**, *28*, 1804975.
- [29] Y. Liang, Y. Yao, *Joule* **2018**, *2*, 1690.
- [30] Z. Song, H. Zhou, *Energy Environ. Sci.* **2013**, *6*, 2280.
- [31] Y. Lu, Q. Zhang, L. Li, Z. Niu, J. Chen, *Chem* **2018**, *4*, 2786.
- [32] Q. Zhao, Y. Lu, J. Chen, *Adv. Energy Mater.* **2017**, *7*, 1601792.
- [33] Z. Tie, L. Liu, S. Deng, D. Zhao, Z. Niu, *Angew. Chem. Int. Ed.* **2020**, *59*, 4920.
- [34] X. Wang, C. Bommier, Z. Jian, Z. Li, R. S. Chandrabose, I. A. Rodriguez-Perez, P. A. Greaney, X. Ji, *Angew. Chem. Int. Ed.* **2017**, *56*, 2909.
- [35] Z. Lin, H. Y. Shi, L. Lin, X. Yang, W. Wu, X. Sun, *Nat. Commun.* **2021**, *12*, 4424.
- [36] S. Muensch, A. Wild, C. Friebel, B. Häupler, T. Janoschka, U. S. Schubert, *Chem. Rev.* **2016**, *116*, 9438.
- [37] H. Kim, J. E. Kwon, B. Lee, J. Hong, M. Lee, S. Y. Park, K. Kang, *Chem. Mater.* **2015**, *27*, 7258.
- [38] Y. Lu, Y. Lu, Z. Niu, J. Chen, *Adv. Energy Mater.* **2018**, *8*, 1702469.
- [39] K. Koshiba, N. Sano, K. Oyaizu, H. Nishide, *Macromol. Chem. Phys.* **2009**, *210*, 1989.
- [40] S. Zheng, D. Shi, D. Yan, Q. Wang, T. Sun, T. Ma, L. Li, D. He, Z. Tao, J. Chen, *Angew. Chem. Int. Ed.* **2022**, *61*, e202117511.
- [41] Z. Guo, Y. Ma, X. Dong, J. Huang, Y. Wang, Y. Xia, *Angew. Chem. Int. Ed.* **2018**, *57*, 11737.
- [42] Y. Luo, F. Zheng, L. Liu, K. Lei, X. Hou, G. Xu, H. Meng, J. Shi, F. Li, *ChemSusChem* **2020**, *13*, 2239.
- [43] W. Wu, H.-Y. Shi, Z. Lin, X. Yang, C. Li, L. Lin, Y. Song, D. Guo, X.-X. Liu, X. Sun, *Chem. Eng. J.* **2021**, *419*, 129659.
- [44] M. Yao, K. Okuno, T. Iwaki, S. Tanase, K. Harada, M. Kato, K. Emura, T. Sakai, *J. Power Sources* **2007**, *171*, 1033.
- [45] M. Yao, K. Okuno, T. Iwaki, T. Awazu, T. Sakai, *J. Power Sources* **2010**, *195*, 2077.
- [46] L. Wang, X. Li, T. Guo, X. Yan, B. K. Tay, *Int. J. Hydrogen Energy* **2014**, *39*, 7876.
- [47] Y. Xia, D. Zhu, S. Si, D. Li, S. Wu, *J. Power Sources* **2015**, *283*, 125.
- [48] M. Sima, T. Visan, M. Buda, *J. Power Sources* **1995**, *56*, 133.
- [49] S. Zhang, W. Zhao, H. Li, Q. Xu, *ChemSusChem* **2020**, *13*, 188.
- [50] B. Häupler, C. Rössel, A. M. Schwenke, J. Winsberg, D. Schmidt, A. Wild, U. S. Schubert, *NPG Asia Mater.* **2016**, *8*, e283.
- [51] Y. Liu, L. Xie, W. Zhang, Z. Dai, W. Wei, S. Luo, X. Chen, W. Chen, F. Rao, L. Wang, Y. Huang, *ACS Appl. Mater. Interfaces* **2019**, *11*, 30943.
- [52] X. Li, X. Xie, R. Lv, B. Na, B. Wang, Y. He, *Energy Technol.* **2019**, *7*, 1801092.
- [53] N. Patil, C. Cruz, D. Ciurdur, A. Mavrandakis, J. Palma, R. Marcilla, *Adv. Energy Mater.* **2021**, *11*, 2100939.
- [54] H. Yu, G. Liu, M. Wang, R. Ren, G. Shim, J. Y. Kim, M. X. Tran, D. Byun, J. K. Lee, *ACS Appl. Mater. Interfaces* **2020**, *12*, 5820.
- [55] F. Trinidad, M. C. Montemayor, E. Fatás, *J. Electrochem. Soc.* **2019**, *138*, 3186.
- [56] C. Kim, B. Y. Ahn, T. S. Wei, Y. Jo, S. Jeong, Y. Choi, I. D. Kim, J. A. Lewis, *ACS Nano* **2018**, *12*, 11838.
- [57] S. Li, I. Sultana, Z. Guo, C. Wang, G. G. Wallace, H.-K. Liu, *Electrochim. Acta* **2013**, *95*, 212.
- [58] B. N. Grgur, M. M. Gvozdenović, J. Stevanović, B. Z. Jugović, V. M. Marinović, *Electrochim. Acta* **2008**, *53*, 4627.
- [59] X. Yue, H. Liu, P. Liu, *Chem. Commun.* **2019**, *55*, 1647.
- [60] Z. Cai, J. Guo, H. Yang, Y. Xu, *J. Power Sources* **2015**, *279*, 114.
- [61] M. J. Park, H. Yaghoobnejad Asl, A. Manthiram, *ACS Energy Lett.* **2020**, *5*, 2367.
- [62] K. W. Nam, H. Kim, Y. Beldjoudi, T. W. Kwon, D. J. Kim, J. F. Stoddart, *J. Am. Chem. Soc.* **2020**, *142*, 2541.
- [63] Y. Yamada, J. Wang, S. Ko, E. Watanabe, A. Yamada, *Nat. Energy* **2019**, *4*, 269.
- [64] K. Xu, *Chem. Rev.* **2014**, *114*, 11503.
- [65] H. Y. Shi, Y. J. Ye, K. Liu, Y. Song, X. Sun, *Angew. Chem. Int. Ed.* **2018**, *57*, 16359.
- [66] J. Zhang, D. Shan, S. Mu, *J. Power Sources* **2006**, *161*, 685.
- [67] C. Chen, X. Hong, A. Chen, T. Xu, L. Lu, S. Lin, Y. Gao, *Electrochim. Acta* **2016**, *190*, 240.
- [68] C. Chen, Z. Gan, C. Xu, L. Lu, Y. Liu, Y. Gao, *Electrochim. Acta* **2017**, *252*, 226.
- [69] W. Du, J. Xiao, H. Geng, Y. Yang, Y. Zhang, E. H. Ang, M. Ye, C. C. Li, *J. Power Sources* **2020**, *450*, 227716.
- [70] H. Yao, Q. Li, M. Zhang, Z. Tao, Y. Yang, *Chem. Eng. J.* **2020**, *392*, 123653.
- [71] S. Mu, Q. Shi, *Synth. Met.* **2016**, *221*, 8.
- [72] X. Wang, L. Chen, F. Lu, J. Liu, X. Chen, G. Shao, *ChemElectroChem* **2019**, *6*, 3644.
- [73] L. Sieuw, A. Jouhara, É. Quarez, C. Auger, J.-F. Gohy, P. Poizot, A. Vlad, *Chem. Sci.* **2019**, *10*, 418.
- [74] J. Xie, F. Yu, J. Zhao, W. Guo, H.-L. Zhang, G. Cui, Q. Zhang, *Energy Storage Mater.* **2020**, *33*, 283.
- [75] Y. Wang, C. Wang, Z. Ni, Y. Gu, B. Wang, Z. Guo, Z. Wang, D. Bin, J. Ma, Y. Wang, *Adv. Mater.* **2020**, *32*, e2000338.
- [76] M. Tang, S. Zhu, Z. Liu, C. Jiang, Y. Wu, H. Li, B. Wang, E. Wang, J. Ma, C. Wang, *Chem* **2018**, *4*, 2600.
- [77] G. Dawut, Y. Lu, L. Miao, J. Chen, *Inorg. Chem. Front.* **2018**, *5*, 1391.
- [78] C. Zhang, J. Holoubek, X. Wu, A. Daniyar, L. Zhu, C. Chen, D. P. Leonard, I. A. Rodriguez-Perez, J. X. Jiang, C. Fang, X. Ji, *Chem. Commun.* **2018**, *54*, 14097.
- [79] Y.-P. Zhu, J. Yin, X. Zheng, A.-H. Emwas, Y. Lei, O. F. Mohammed, Y. Cui, H. N. Alshareef, *Energy Environ. Sci.* **2021**, *14*, 4463.
- [80] F. Wang, O. Borodin, T. Gao, X. Fan, W. Sun, F. Han, A. Faraone, J. A. Dura, K. Xu, C. Wang, *Nat. Mater.* **2018**, *17*, 543.
- [81] Q. Zheng, Y. Yamada, R. Shang, S. Ko, Y.-Y. Lee, K. Kim, E. Nakamura, A. Yamada, *Nat. Energy* **2020**, *5*, 291.
- [82] Y. Yamada, K. Usui, K. Sodeyama, S. Ko, Y. Tateyama, A. Yamada, *Nat. Energy* **2016**, *1*, 16129.
- [83] Q. Zheng, S. Miura, K. Miyazaki, S. Ko, E. Watanabe, M. Okoshi, C. P. Chou, Y. Nishimura, H. Nakai, T. Kamiya, T. Honda, J. Akikusa, Y. Yamada, A. Yamada, *Angew. Chem. Int. Ed.* **2019**, *58*, 14202.
- [84] L. Suo, O. Borodin, T. Gao, M. Olgquin, J. Ho, X. Fan, C. Luo, C. Wang, K. Xu, *Science* **2015**, *350*, 938.
- [85] L. Suo, Y. S. Hu, H. Li, M. Armand, L. Chen, *Nat. Commun.* **2013**, *4*, 1481.
- [86] J. Yue, L. Lin, L. Jiang, Q. Zhang, Y. Tong, L. Suo, Y. S. Hu, H. Li, X. Huang, L. Chen, *Adv. Energy Mater.* **2020**, *10*, 2000665.
- [87] S. Liu, J. Mao, W. K. Pang, J. Vongsivut, X. Zeng, L. Thomsen, Y. Wang, J. Liu, D. Li, Z. Guo, *Adv. Funct. Mater.* **2021**, *31*, 2104281.
- [88] J. Zhao, J. Zhang, W. Yang, B. Chen, Z. Zhao, H. Qiu, S. Dong, X. Zhou, G. Cui, L. Chen, *Nano Energy* **2019**, *57*, 625.
- [89] J. Xie, Z. Liang, Y. C. Lu, *Nat. Mater.* **2020**, *19*, 1006.
- [90] W. Yang, X. Du, J. Zhao, Z. Chen, J. Li, J. Xie, Y. Zhang, Z. Cui, Q. Kong, Z. Zhao, C. Wang, Q. Zhang, G. Cui, *Joule* **2020**, *4*, 1557.

- [91] V. Verma, S. Kumar, W. Manalastas, M. Srinivasan, *ACS Energy Lett.* **2021**, *6*, 1773.
- [92] J. Hao, B. Li, X. Li, X. Zeng, S. Zhang, F. Yang, S. Liu, D. Li, C. Wu, Z. Guo, *Adv. Mater.* **2020**, *32*, e2003021.
- [93] L. Ma, T. P. Pollard, Y. Zhang, M. A. Schroeder, M. S. Ding, A. V. Cresce, R. Sun, D. R. Baker, B. A. Helms, E. J. Maginn, C. Wang, O. Borodin, K. Xu, *Angew. Chem. Int. Ed.* **2021**, *60*, 12438.
- [94] L. Yan, X. Zeng, Z. Li, X. Meng, D. Wei, T. Liu, M. Ling, Z. Lin, C. Liang, *Mater. Today* **2019**, *13*, 323.
- [95] Y. Zhang, Q. Wang, S. Bi, M. Yao, F. Wan, Z. Niu, *Nanoscale* **2019**, *11*, 17630.
- [96] P. Liu, R. Lv, Y. He, B. Na, B. Wang, H. Liu, *J. Power Sources* **2019**, *410–411*, 137.
- [97] H. Cao, F. Wan, L. Zhang, X. Dai, S. Huang, L. Liu, Z. Niu, *J. Mater. Chem. A* **2019**, *7*, 11734.
- [98] S. Liu, R. Zhang, J. Mao, Y. Zhao, Q. Cai, Z. Guo, *Sci. Adv.* **2022**, *8*, eabn5097.
- [99] Y. Wang, Z. Wang, F. Yang, S. Liu, S. Zhang, J. Mao, Z. Guo, *Small* **2022**, e2107033. DOI: 10.1002/smll.202107033
- [100] T. Sun, X. Yuan, K. Wang, S. Zheng, J. Shi, Q. Zhang, W. Cai, J. Liang, Z. Tao, *J. Mater. Chem. A* **2021**, *9*, 7042.
- [101] Q. Zhang, Y. Ma, Y. Lu, L. Li, F. Wan, K. Zhang, J. Chen, *Nat. Commun.* **2020**, *11*, 4463.
- [102] J. Hao, L. Yuan, C. Ye, D. Chao, K. Davey, Z. Guo, S. Z. Qiao, *Angew. Chem., Int. Ed.* **2021**, *60*, 7366.
- [103] N. Wang, Y. Yang, X. Qiu, X. Dong, Y. Wang, Y. Xia, *ChemSusChem* **2020**, *13*, 5556.

Manuscript received: April 27, 2022

Revised manuscript received: June 18, 2022

Accepted manuscript online: June 26, 2022

Version of record online: July 7, 2022